

# RSC Advances



This is an *Accepted Manuscript*, which has been through the Royal Society of Chemistry peer review process and has been accepted for publication.

*Accepted Manuscripts* are published online shortly after acceptance, before technical editing, formatting and proof reading. Using this free service, authors can make their results available to the community, in citable form, before we publish the edited article. This *Accepted Manuscript* will be replaced by the edited, formatted and paginated article as soon as this is available.

You can find more information about *Accepted Manuscripts* in the [Information for Authors](#).

Please note that technical editing may introduce minor changes to the text and/or graphics, which may alter content. The journal's standard [Terms & Conditions](#) and the [Ethical guidelines](#) still apply. In no event shall the Royal Society of Chemistry be held responsible for any errors or omissions in this *Accepted Manuscript* or any consequences arising from the use of any information it contains.

## Ceria nanoparticles for the treatment of Parkinson-like diseases induced by chronic manganese intoxication

Alessandra Pinna<sup>a</sup>, Luca Malfatti<sup>a</sup>, Grazia Galleri<sup>b</sup>, Roberto Manetti<sup>b</sup>, Sara Cossu<sup>b</sup>, Gaia Rocchitta<sup>b</sup>, Rossana Migheli<sup>b</sup>, Pier Andrea Serra<sup>b\*</sup> and Plinio Innocenzi<sup>a\*</sup>

<sup>a</sup> *Laboratorio di Scienza dei Materiali e Nanotecnologie, CR-INSTM, Università di Sassari, Palazzo Pou Salid, Piazza Duomo 6, 07041 Alghero (SS), Italy.*

<sup>b</sup> *Dipartimento di Medicina Clinica e Sperimentale, Università di Sassari, 07100 Sassari, Italy.*

*\*corresponding authors: Pier Andrea Serra; Università di Sassari, viale S. Pietro 43 B, 07100*

*Sassari Italy, fax number: +39 079 228525; E-mail address:*

*paserra@gmail.com.*

*Plinio Innocenzi; Università di Sassari, Laboratorio di Scienza dei Materiali e Nanotecnologie, CR-INSTM, Palazzo Pou Salid, Piazza Duomo 6, 07041*

*Alghero (SS), Italy, fax number: +39 079 9720420; E-mail address:*

*plinio@uniss.it.*

### Abstract

Ceria nanoparticles with controlled size have been studied as antioxidant agent for the *in-vitro* protection of catecholaminergic cells (PC12) exposed to manganese, which is responsible for an occupational form of Parkinson-like disease. The nanoparticle internalization has been followed by Raman and confocal microscopy while the effect of nanoceria concentration in the cell metabolism has been assessed by MTT and trypan blue assay. With the perspective to develop an innovative combined treatment, nanoceria has been tested either alone or in association with L-DOPA showing a significant effect in reducing the oxidative stress due to manganese chloride. Finally, to study the

protective role of nanoceria on the metabolism of catecholamines, the intracellular concentration of dopamine and its metabolites have been monitored by liquid chromatography with electro-chemical detection in control and nanoparticle-exposed cells as a function of the nanoceria dosing. The results show a protective role of nanoceria both on PC12 cells survival and dopamine metabolism, which makes this class of nanoparticles a potential candidate for the treatment of Parkinson-like diseases induced by chronic manganese intoxication.

**Keywords:** Nanoceria; Parkinson like diseases; antioxidant; magnesium chloride; L-DOPA

## 1. Introduction

Parkinson like disease (PLD) symptoms are produced by severe neurodegenerative processes caused by the interplay of a number of factors, such as environmental or genetic risk, age, mitochondrial dysfunction and other conditions leading to a reactive oxygen species (ROS) overproduction.<sup>1</sup> Among the different causes, oxidative stress has been widely believed to be an important pathogenetic mechanism of neuronal death in the disease, although it is still not clear whether it is an initial event causing cell death or a consequence of the disease. The causes of the oxidative stress can be found in a large variety of sources and, in some cases, the presence of PLD symptoms can be correlated with the exposure to transition metals such as copper, lead and manganese.<sup>2</sup> In particular, chronic manganese intoxication in humans is responsible for early psychotic disorder that is later followed by permanent degenerative damage in the nigrostriatal system, resulting in a PLD. It is well known that manganese may stimulate dopamine (DA) autoxidation in the dopaminergic neuron, resulting in an increase of the quinones levels. The generated quinones are thought to mediate toxicity by covalently binding to nucleophilic groups of biological macromolecules.<sup>3</sup>

In virtue of the multiplicity of its oxidation states (commonly +2, +3, +4, +6 and +7), manganese shows a wide range of chemical interactions which becomes even more complex in a biological

environment. This means that Mn can mimic other ions and enter into the brain through different carriers. As well as damage to the dopaminergic system, Mn induces mitochondrial dysfunction, impairment of cellular energy metabolism, glial activation, neuroinflammation and deep changes in synaptic transmission and astrocytes-neurons cross-talk;<sup>4</sup> all these factors contribute to the onset of the PLD.

The administration of L-3,4-dihydroxyphenylalanine (L-DOPA), the natural precursor of dopamine in catecholaminergic neurons, is the most widely used treatment for PD-like syndrome; the alleviation of the symptoms related to the disease are due to a replenishment of DA in the surviving neurons. However, although many of the symptoms of PLD can be relieved, the therapy is not curative and dopaminergic cells continue to die in patients receiving L-DOPA. In fact L-DOPA can undergo autoxidation and enzymatic oxidation, generating a variety of cytotoxic ROS, including superoxide, hydrogen peroxide, semiquinones, and quinones<sup>5,6</sup> which may further load the preexisting condition of oxidative stress. Since L-DOPA induces oxidative stress-mediated apoptosis in cultured neuronal cells, the inappropriate L-DOPA-induced activation of apoptosis might have a role in neuronal death in PLD syndrome.<sup>7</sup>

In the last years, Cerium oxide ( $\text{CeO}_2$ ) gained increasing interest for its capability of neutralizing and reducing ROS; this property is related to the presence of oxygen vacancies on the  $\text{CeO}_2$  surface, which allows Ce ions to flip-flop between two oxidation states.<sup>8</sup> When ROS interact with  $\text{CeO}_2$  surface, the  $\text{Ce}^{3+}$  ions are oxidized to  $\text{Ce}^{4+}$  neutralizing the radicals; afterwards,  $\text{Ce}^{4+}$  centers reduce again their oxidation state to  $\text{Ce}^{3+}$  by reaction with  $\text{H}^+$ .<sup>9,10</sup> Since the antioxidant process is strictly correlated to the surface property, this effect becomes of extreme relevance when cerium oxide is used in form of nanosized particles, also called nanoceria.<sup>11,12,13</sup> When nanoceria is used in a biological environment, such as in cell cultures or animal models, the nanoparticles act as radical scavengers mimicking the role of superoxide dismutase and catalase.

Compared to organic exogenous antioxidants, which are limited by chemical instability,<sup>14</sup> nanoceria shows the major advantage of an auto-regenerative process.<sup>15</sup> In fact, the switching of cerium

oxidation states allows restoring the radical scavenging properties without continuously dosing the drug, as in the case of organic exogenous antioxidants. In addition, antioxidant processes triggered by nanoceria provide an effective protection not only against ROS, but also towards other reactive molecules, such as nitrogen-based species (RNS)<sup>16</sup> enabling a simultaneous quenching of dangerous metabolic byproducts.

In this work, nanoceria has been tested as an adjuvant drug in the treatment of PLD syndrome which is an ideal model to test the nanoceria properties applied to neurodegenerative syndromes. The protective effects of nanoceria on manganese- and L-DOPA- induced cytotoxicity have been evaluated in nerve pheochromocytoma cell line, PC12 cells. This cell line exhibits several physiological properties which are characteristic of dopaminergic neurons and therefore it is a good system for the study of oxidative stress in dopamine-containing cells.

## 2. Materials and Methods

### 2.1. Materials

Cerium(III) nitrate hexahydrate ( $\text{Ce}(\text{NO}_3)_3 \cdot 6\text{H}_2\text{O}$ , ABCR 99.9%), urea ( $\text{CH}_4\text{N}_2\text{O}$ , Aldrich 99%), 2-propanol (99.7%, Carlo Erba), 1M hydrochloric acid (HCl, Aldrich), 5M aqueous ammonia ( $\text{NH}_4\text{OH}$ , Aldrich), 3 aminopropyltriethoxysilane (APTES,  $\text{NH}_2(\text{CH}_2)_3\text{Si}(\text{OC}_2\text{H}_5)_3$ , 99%, Aldrich), fluorescein isothiocyanate isomer I (FITC,  $\text{C}_{21}\text{H}_{11}\text{NO}_5\text{S}$ , 90%, Aldrich), ethanol (EtOH, Fluka 99.8%), acetone (Aldrich 99.5%) and N,N-dimethylformamide (DMF,  $\text{C}_3\text{H}_7\text{NO}$ , Aldrich) were used as received without further purification.

Dulbecco's modified Eagle's medium (DMEM/F-12, HEPES, no phenol red), horse and fetal bovine (FBS) serum were purchased from Life Technologies, L-3,4-dihydroxyphenylalanine (L-DOPA, 98%) from Sigma-Aldrich (Milan, Italy) and manganese chloride ( $\text{MnCl}_2$ ) from Merck (Darmstadt, Germany).

3-(4,5-dimethyl- thiazol-2-yl)-2,5-diphenyltetrazolium bromide for MTT assay (97.5%), phosphate buffer saline solution (PBS, 0.2 $\mu$ m filtered), trypan blue (0.4%), gelatin, 4,6-diamidino-2-phenylindole dihydrochloride (DAPI, 98%), 0.5 M Citric acid (99.5%), 1.0 M sodium acetate (NaAc, 99%), 12.5 mM ethylenediaminetetraacetic acid (EDTA, 98.5%), methanol 10% (MeOH, 99.93%), sodium octylsulphate ( $\text{CH}_3(\text{CH}_2)_7\text{OSO}_3\text{Na}$ , pH 3.0, 95%), annexin V-fluorescein isothiocyanate (FITC) propidiumiodide (PI), Annexine V-FITC kit (MACS Mylteny Biotec), and trypan blue 0.4% were purchased from Sigma Aldrich.

## 2.2. Methods

### 2.2.1. Synthesis of Nanoceria

Urea was used as coordinating agent,  $\text{NH}_4\text{OH}$  and  $\text{Ce}(\text{NO}_3)_3$  as inorganic precursors.  $7 \times 10^3$  mg of  $\text{Ce}(\text{NO}_3)_3 \cdot 6\text{H}_2\text{O}$  were dissolved in 20 ml of 2-propanol, then 0.5 ml of hydrochloric acid were added to it and left under stirring until a homogeneous solution was obtained. In a separate vial,  $2 \times 10^3$  mg of urea and 0.5 ml of HCl were dissolved in 20 ml of 2-propanol and left under stirring for 5 min. The urea solution was then added, dropwise, to the  $\text{Ce}(\text{NO}_3)_3$  solution under stirring, and soon after 14 ml of  $\text{NH}_4\text{OH}(\text{aq})$  were added to the mixture to form a precipitate that was exposed to microwaves (4 times at 600 W for 10 s), washed with water and centrifuged at 10000 rpm. A light yellow milky dispersion was obtained that was then diluted with water to reach a concentration of 56 mg  $\text{CeO}_2$  per ml (nanoceria stock suspension).

### 2.2.2. Functionalization of Ceria Nanoparticles with fluorescein isothiocyanate (FITC)

Nanoceria was firstly functionalized with 3-aminopropyltriethoxysilane by mixing 200 mg of nanoceria with 3 ml of APTES and 50 ml of EtOH at room temperature under stirring. The amino-functionalized nanoceria ( $\text{NH}_2$ -nanoceria) was washed with EtOH and centrifuged at 10000 rpm. 4 mg of nanoceria were then re-suspended in 0.5 ml of DMF, mixed with 0.5 ml of 2 mg/ml FITC in DMF and stirred at room temperature for 4 h. The FITC- $\text{NH}_2$  nanoceria were washed once with

acetone and twice with water and centrifuged at 10000 rpm. The orange precipitate was diluted with water to reach a concentration of 22 mg per ml (FITC-NH<sub>2</sub>-nanoceria).

### 2.2.3. Nanoparticles characterization

A Vertex 70 Bruker spectrophotometer in the 400- 4000 cm<sup>-1</sup> range, with a resolution of 4 cm<sup>-1</sup> was used for Fourier transform infrared (FTIR) spectroscopy. Nanoceria, NH<sub>2</sub>-nanoceria and FITC-NH<sub>2</sub>-nanoceria solutions were casted onto a silicon wafer and then measured in transmission; bare silicon was used as a background reference. The FTIR spectra were analyzed in the 3700 - 400 cm<sup>-1</sup> region; the baseline was corrected using a concave rubberband function with OPUS 7 software.

X-ray diffraction (XRD) pattern of CeO<sub>2</sub> nanoparticles was collected by a Bruker D8 "Discover" in grazing incidence geometry with a Cu K $\alpha$  line ( $\lambda = 1.54056 \text{ \AA}$ ); the X-ray generator worked at a power of 40 kV and 40 mA. The patterns were recorded in 2 $\theta$  mode ranging from 20 to 80° with a step size of 0.02° and a scan speed of 0.5 s until an optimal signal-to-noise ratio was achieved. The average crystallite size  $D$  was calculated from the broadening of the X-ray line (1 1 1) using Scherrer's equation [17] and EVA program.

Transmission electron microscopy (TEM) images were obtained by using a Hitachi H-70000 microscope equipped with a tungsten cathode operating at 125 kV. For sample measurements, few drops of nanoceria were cast on a carbon coated copper grid and dried for observations.

### 2.2.4. Cell culture and viability assay

PC12 cells (ATCC CRL-1721), derived from a transplantable rat pheochromocytoma, are a valuable model for neuronal differentiation, mimicking any features of central dopaminergic neurons including dopamine production.<sup>18</sup>

PC12 cells were maintained at 37°C in 60-mm plastic culture plates in an atmosphere of 5% CO<sub>2</sub>/95% humidified air. The formulation of the culture medium was prepared as follows: Dulbecco's modified Eagle's medium (DMEM) – F12 supplemented with 10% horse serum and 5% fetal bovine serum.

For viability testing PC12 cells were exposed or not exposed (control) for 48 hours to different concentrations of ceria nanoparticles (5 – 5000  $\mu\text{g/ml}$ ) in 24-well plates ( $10^5$  cells per well).

To evaluate ceria neuroprotective effect, PC12 cells were pretreated for 24 h with 10, 20 and 50  $\mu\text{g/ml}$  of ceria and then  $\text{MnCl}_2$  and/or L-DOPA were added at the concentration of 750  $\mu\text{M}$  and 20  $\mu\text{M}$  respectively for further 24 h. All experiments were done in triplicate. Cell viability was then assessed by the 3-(4, 5-dimethyl- thiazol-2-yl)-2, 5, diphenyltetrazolium bromide (MTT) assay. In this assay, viable cells convert the soluble dye MTT to insoluble (in aqueous media) blue formazan crystals. In details, 200  $\mu\text{l}$  of MTT [5 mg/ml stock solution in phosphate buffered saline (PBS)] was added to 1 ml of medium and incubated at 37°C for 4 h. The MTT was removed and the cells rinsed with PBS and centrifuged at 4000 rpm for 20 min. The resulting pellet was dissolved in 2 ml of isopropanol and centrifuged at 4000 rpm for 5 min. Finally the supernatant color was read at 600 nm using a Bauty Diagnostic Microplate Reader. A calibration standard curve was achieved before each experiment using different cells concentration.

#### *2.2.5. PC12 apoptosis assessment*

PC12 cells were seeded in a 24-well plate, pretreated for 24 h with 10, 20, 50 and 100  $\mu\text{g/ml}$  of ceria, at concentration of  $1.2 \times 10^5$  cells/well and cultured overnight. Then  $\text{MnCl}_2$  (750  $\mu\text{M}$ ) and/or L-DOPA (20  $\mu\text{M}$ ) were added to cells and incubated for further 24 h. After incubation the cells were washed with annexin binding buffer. Cell apoptosis was assessed using annexin V-fluorescein isothiocyanate (FITC) apoptosis detection kit (BD Biosciences, San Diego, USA). Cells were incubated with FITC-labeled annexin V and propidiumiodide (PI) for 15 minutes in dark at room temperature (20–25°C). The cell percentage showing annexin V+/PI- and annexin V+/PI+ was used to evaluate apoptotic cells by a FACS Calibur with Cell Quest 6.0 software (BD Bioscience); 10000 events were collected for each experiment.

#### *2.2.6. Evaluation of Ceria Uptake into PC12 cells*

PC12 cells were exposed or not exposed (control) for 48 hours to different concentrations of FITC- $\text{NH}_2$ -nanoceria (20 - 50 - 100  $\mu\text{g/ml}$ ) in 24-well plates ( $1.2 \times 10^5$  cells per well). After incubation, the

cells were washed 3 times with PBS and resuspended in Dulbecco's modified Eagle's medium containing 0.25% w/w of trypan blue.

The uptake of FITC-NH<sub>2</sub>-nanoceria into PC12 cells was evaluated by FACS Calibur flow cytometer (Becton Dickinson, FACScalibur<sup>TM</sup>, USA) and Raman spectroscopy. The side scatter data obtained by flow cytometry were analyzed using CELL Quest 6.0 software (BD Bioscience).<sup>19</sup>

For Raman analysis PC12 cells were seeded on gelatin (1 mg/ml in sterile milliQ water) coated glass coverslips at 10<sup>5</sup> cells/ml and cultured overnight. Then cells were treated with ceria nanoparticles (40 µg/ml) for another 24 h. After that, cells were rinsed two times with PBS and glass coverslips were placed and sealed on a microscope slide. The intracellular localization was detected by a Bruker Senterra confocal Raman microscope (50× magnification for optical images) working with a laser excitation wavelength of 532 nm at 12 mW of nominal power. Raman imaging maps were obtained by selecting the 50× objective, and an defining an array of 598 points in order to cover an area of 25 × 22 µm with a step of 1.0 µm. Each spectrum of the map was recorded by averaging 10 acquisitions of 3s.

#### 2.2.7. Confocal microscopy

PC12 cells were seeded on gelatin (1 mg/ml in sterile milliQ water) coated glass coverslips at 10<sup>5</sup> cells/ml and cultured overnight. Then, the cells were treated with FITC-NH<sub>2</sub> nanoceria (10 or 20 µg/ml) for another 24 h. Afterwards, the cells were rinsed two times with PBS and stained with DAPI (5 µg/ml in PBS) for 15 minutes, protecting them from light. Cells were then rinsed one time with PBS and sealed on microscope slides.

Samples were observed with a Leica Microscope, equipped with a Leica Confocal Laser System C2s. The images were analysed by Leica Application Suite Advance Fluorescence Lite (LAS AF) program.

#### 2.2.8. Chromatographic analysis

High performance liquid chromatography with electro-chemical detection (HPLC-EC) was used to quantify DA, dihydroxyphenylacetic acid (DOPAC), homovanillic acid (HVA), 3-

Methoxytyramine (3-MT) using an Alltech 426 HPLC pump equipped with a Rheodyne injector, column 15 cm 64.6 mm i.d. Alltech Adsorbosphere C18 5U, electrochemical detector Antec CU-04-AZ and Varian Star Chromatographic Workstation. Citric acid 0.5 M, Na acetate 1.0 M, EDTA 12.5 mM, MeOH 10% and sodium octylsulphate 650 mg l<sup>-1</sup> (pH 3.0) was the mobile phase; the flow rate was 1×3 ml min<sup>-1</sup>.<sup>20</sup>

### 2.2.9. Statistical analysis

All in vitro data derive from at least three independent experiments and results are expressed as mean values with 95% confidence intervals. The statistical significance of differential findings between experimental and control groups was estimated by paired or unpaired t-test in Graph-Pad Prism 5.0 software (GraphPad Software, Inc, San Diego, CA, USA). These findings were considered significant if two-tailed P values were <0.05.

## 3. Results and Discussion

### 3.1. Nanoceria characterization and functionalization

Nanoceria has been synthesized by a microwave treatment, a process that allows for a fast fabrication of well-dispersed nanoparticles in water without using thermal annealing.<sup>21</sup> After synthesis, the nanoparticles (NPs) have been characterized by XRD and TEM to correlate their chemical-physical features with the functional properties. The XRD pattern in the 20°–80° 2θ angular range (**Fig. 1**) has been indexed according to the cubic fluorite structure of cerianite (JCPDS: 34–0394). The crystal size of nanoparticle, calculated by Scherrer's equation, is around 9 ± 1 nm. The size is in accordance with nanoparticle diameter as measured by bright field TEM characterization (8.5 ± 1.3 nm) suggesting that the nanoparticles are formed by single crystals. (See ESI, **Fig. S1**).

Infrared spectroscopy has been used to characterize the functionalization of ceria NPs with the fluorophore FITC. **Fig. 2a** shows the spectrum of pure NPs in the 3700–400 cm<sup>-1</sup> range; the broad

band peaked at  $3450\text{ cm}^{-1}$  is assigned to the symmetric stretching of the hydroxyl group on the nanoparticle surface<sup>22</sup> while the band at  $1600\text{ cm}^{-1}$  is due to residual water. The bands below  $1460\text{ cm}^{-1}$  ( $1465$ ,  $1319$  and  $1045\text{ cm}^{-1}$  respectively) have been attributed to the formation of  $\text{CO}_3^{2-}$  on the particle surface as a consequence of the interaction between  $\text{CeO}_2$  and atmospheric  $\text{CO}_2$ .<sup>23</sup> Remarkably, the presence of these bands is strongly reduced if the particles are kept in solution.

Functionalization with FITC has been obtained through chemical modification of the NPs surface with an organosilane linker (aminopropyl trimethoxysilane, APTES) containing a  $-\text{NH}_2$  terminal group. **Fig. 2b** shows the change induced in the infrared spectra by the successful APTES modification. The broad band peaked at  $3450\text{ cm}^{-1}$  decreases in absorbance, in accordance to the reduced amount of hydroxyls available on the NPs surface, while the introduction of aminosilane groups is confirmed by the appearance of three bands: the first one, at  $1556\text{ cm}^{-1}$ , attributed to NH bending of the amide bond; the second one, peaked at  $2966\text{ cm}^{-1}$ , due to  $\text{CH}_3$  stretching mode and the third one, at  $2932\text{ cm}^{-1}$ , related to  $\text{CH}_2$  stretching. The broad band at  $952\text{ cm}^{-1}$  has been assigned to the Ce–O–Si stretching vibration as a consequence of the covalent bond between APTES and nanoceria.<sup>24</sup> **Fig. 2d** shows the spectrum of the  $\text{NH}_2$  modified nanoceria after functionalization with FITC. By comparing the spectrum of the pure fluorophore, **Fig. 2c**, with that one of the FITC-functionalized nanoparticles, we observe the disappearance of the band relative to the isothiocyanate group  $\text{N}=\text{C}=\text{S}$  (at  $2069\text{ cm}^{-1}$ ) as a result of the coupling with the amine. A comparison between the spectra of **Fig. 2d** and **2c** allows highlighting an increase of the  $\text{CH}_2$  stretching band at  $2930\text{ cm}^{-1}$  attributed to the fluorescent molecule linked to the ceria NPS.<sup>24</sup>

### 3.2. Evaluation of nanoceria uptake and toxicity in PC12 cells

To assess the toxicity of nanoceria, PC12 cells have been exposed to increasing concentrations of nanoparticles (from 0 to  $5000\text{ }\mu\text{g/ml}$ ) and their viability has been assessed by MTT assay. **Fig. 3** shows that nanoceria has not affected cells viability when administered in concentrations from 5 to  $100\text{ }\mu\text{g/ml}$  but starts to become toxic at concentrations higher than  $100\text{ }\mu\text{g/ml}$ . This results in a

statistically significant reduction ( $p < 0.05$ ) of cell viability which gradually decreases in comparison with controls from 75%, at a concentration of 500  $\mu\text{g/ml}$ , down to 57% at a concentration of 4000  $\mu\text{g/ml}$ .

MTT assay has allowed evaluating the maximum nanoparticle concentration that does not induce cellular toxicity. According to these results, a range between 20 and 100  $\mu\text{g/ml}$  has been chosen to evaluate the NPs antioxidant effect by apoptosis assay on a cell culture previously exposed to an oxidative insult.

$\text{MnCl}_2$  at a concentration of 750  $\mu\text{M}$  has been selected as the oxidant agent to simulate the degenerative processes occurring in PDL syndrome caused by chronic manganese intoxication. **Fig. 4** shows a representative flow cytometry profile PI/annexinV performed on cell cultures treated with  $\text{CeO}_2$  and  $\text{MnCl}_2$ . The oxidative insult causes a 27.7% cell apoptosis (**Fig. 4b**) with respect not-treated cells (**Fig. 4a**). However, if cells previously treated with 20  $\mu\text{g/ml}$  of nanoceria, the apoptotic cell percentage dramatically drops to 3.8% (**Fig. 4d**). **Fig. 4c** shows the effect of nanoceria administration compared to the control; the data show no significant variations in the cell apoptosis, in accordance to the MTT assay and previous studies.<sup>25</sup> The experiments have been reproduced in triplicate as a function of the NPs concentration and the averaged results have been reported in a bar plot (**Fig. 4e**).  $\text{MnCl}_2$  causes  $28 \pm 3.5\%$  of apoptosis, while the injury decreases in the cells pre-treated with nanoceria; the PC12 cultures treated with 10, 20, 50 and 100  $\mu\text{g/ml}$  of  $\text{CeO}_2$ , in fact, show a percentage in apoptosis of  $3\% \pm 0.5$ ,  $4.5\% \pm 0.5$ ,  $2.8\% \pm 0.5$  and  $3\% \pm 0.4$ , respectively. The addition of L-DOPA to the treatment groups does not cause significant changes in the percentages of cell apoptosis (data not shown).

Flow cytometry with fluorescent nanoceria has been used to assess whether the  $\text{CeO}_2$  antioxidant effect occurred indirectly, through ROS quenching in the extracellular environment, or directly, as a consequence of intracellular uptake. **Fig. 5** shows the fluorescence intensity of the cells as a function of the nanoceria concentration; the median fluorescence intensity (MFI) increases from 9.97 to 137.16 a. u. with the increase of NPs concentration from 20  $\mu\text{g/ml}$  up to 100  $\mu\text{g/ml}$ . The cell

cultures have been treated with trypan blue before cytometry, so that the fluorescence signal can be univocally attributed to NPs inside the cells. A higher nanoceria concentration causes an increase in the median fluorescence intensity of the cells; this indicates that there is an almost linear correlation between the amount of NPs incubated with the PC12 cultures and the number of nanoparticles uptaken by the cells.

PC12 cells, fixed on a glass with a gelatin from bovine skin, have been analyzed by Raman imaging to confirm the ceria uptake (**Fig. 6a**). The image in false color scale has been obtained by sampling the area shown in **Fig. 6b** with a Raman microscope and integrating the band peaked at  $465\text{ cm}^{-1}$ , which is the main absorption band of nanoceria in water **Fig. 6c**.<sup>26</sup> **Fig. 6d** shows the difference in the Raman spectrum when the microscope is sampling an area containing nanoceria (black line), in comparison with the extracellular area, where no particles are detected (red line). The imaging clearly shows the presence of cerium oxide inside the cell due to nanoparticles uptake while no signals attributed to nanoceria are visible in the extracellular environment.

Confocal microscopy has also confirmed the internalization of cerium oxide NPs into PC12 cells **Fig. 7**. After 24 h of incubation with  $20\text{ }\mu\text{g/ml}$  of FITC-nanoceria, the highly fluorescent green spots inside the cytoplasm cells prove the successful internalization. Z-stack and 3D rendering have confirmed that the NPs are effectively inside the cells and not on the cell surface (see **Movie**) while no evidence of NPs in the cell nuclei has been observed.

### 3.3 Effect of nanoceria against $\text{MnCl}_2$ - and $\text{MnCl}_2 + \text{L-DOPA}$ -induced oxidative stress

The most common treatment of PLD syndromes is the administration of L-DOPA, which is the natural precursor of dopamine, however the auto- and enzymatic oxidation of this compound contributes to further increase of the oxidative stress in the cells. We have decided, therefore, to test the effect of administration of nanoceria on PC12 cells previously exposed to oxidative stress induced by  $\text{MnCl}_2$  and potentiated by L-DOPA. The cell viability has been measured both by MTT and trypan blue assay to cross correlate the results obtained by the two techniques (**Fig. 8**). After the

MnCl<sub>2</sub> insult, the viability is 55% and 65% compared to control, as shown by MTT and TB assays, respectively. The difference in these two values can be justified by considering the different outputs of the techniques; MTT measures, in fact, the mitochondrial dehydrogenase activity while the TB assay allows direct staining of the dead cells. A live cell with reduced dehydrogenase activity, therefore, is accounted as "healthy cell" by TB assay although providing a lower contribution in the cell viability as assessed by MTT.

When PC12 cells are pre-treated with increasing amounts of nanoceria, their viability after the MnCl<sub>2</sub> injury results enhanced. In particular, the cell viability raises of 15% with respect to the control after pretreatment with 10 and 20 µg/ml of cerium oxide NPs ( $p < 0.05$ ).

The simultaneous administration of MnCl<sub>2</sub> and L-DOPA shows a cell viability slightly lower but not statistically different from MnCl<sub>2</sub> alone (60% of control) while nanoceria pre-treatment gives a relative protection. However, the range of protective concentrations of ceria is lower during MnCl<sub>2</sub> exposure (10-20 µg/ml) than MnCl<sub>2</sub> + L-DOPA (20-50 µg/ml). Although the ceria-related increase in cell viability is around 10%, both the assays (MTT and TP) give a similar value, indicating that the both cell activity and viability are statistically enhanced ( $p < 0.05$ ).

To evaluate the dopamine (DA) concentration in untreated and nanoceria-treated PC12 cells, we have measured its intracellular concentration and that of its metabolites (dihydroxyphenylacetic acid (DOPAC), 3-Methoxytyramine (3-MT) and homovanillic acid (HVA) by high performance liquid chromatography with electro-chemical detection. **Fig. 9** shows the changes of the intracellular DA and metabolites content after treatments with nanoceria (20 µg/ml), L-DOPA (0.02 mM), MnCl<sub>2</sub> (750 µM) and their combinations. Remarkably, the treatment with ceria does not cause any change in the intracellular amount of neurochemicals. On the contrary, the MnCl<sub>2</sub> insult causes a strong decrease of the neurochemical catabolites which is around 60%, 73% and 68% for DA, DOPAC and 3-MT, respectively. The HVA content appears almost constant, suggesting a strong resistance towards oxidation; an explanation of these responses can be provided considering the oxy-methylation reaction of the molecule. On the contrary, another oxy-methylated molecule (3-

MT) showed a significant decrease after  $\text{MnCl}_2$  exposure; this behavior could be in relationship with the increased auto-oxidation of its metabolic precursor (DA). Similar decrease in DA, DOPAC and 3-MT concentrations has been also observed when  $\text{MnCl}_2$  is used in association with L-DOPA.

The co-treatment of  $\text{MnCl}_2$  with nanoceria induces a significant protection on DA content, resulting in a 29% decrease with respect to the control value, while the DOPAC and 3-MT contents decrease. The protection of nanoceria against oxidation is still present but less pronounced when is used in association L-DOPA; in fact, the simultaneous treatment with  $\text{MnCl}_2$  + nanoceria + L-DOPA causes a loss in DA, DOPAC and 3-MT content of 41%, 69% and 76%, respectively.

The results have shown that the use of nanoceria to neutralize ROS in PLD oxidative processes enhances the therapeutic effects of L-DOPA delaying neuronal cell degeneration. Although the antioxidant properties of nanoceria are not significantly influenced by the pH,<sup>27</sup> its role largely depends on the dimension and concentration. These parameters have to be carefully controlled to achieve protective effects. In fact, nanoceria at concentration of 20  $\mu\text{g/ml}$  has a high protective action towards oxidative stress caused by  $\text{Mn}^{2+}$  ions and auto-oxidation of L-DOPA, while, at concentration higher than 100  $\mu\text{g/ml}$ , the cell viability is compromised. On the other hand, previous studies have shown the importance of controlling the nanoceria dimension; in fact, particles larger than 10 nm exhibit a lower antioxidant activity and enhanced photocatalytic properties.<sup>28</sup> This is the reason why we have carefully kept the nanoparticle dimension below this critical size.

Understanding nanoceria uptake mechanism is also of paramount importance, for this reason we have used two different techniques to observe the nanoparticles within the cellular environment. At the optimized nanoceria concentration, the nanoparticles result efficiently internalized in the cytoplasm of PC12 cells. However no evidence of nanoparticles uptake in the cell nuclei has been observed, avoiding potential damaging of the DNA.

Interestingly, the results of flow cytometry indicate that nanoceria itself is likely able of reducing the natural apoptosis ratio of the untreated cells; in fact the nanoceria pre-treated cells insulted by MnCl<sub>2</sub> show an even lower percentage apoptosis than the control. On the other hand, it is also remarkable that L-DOPA does not protect the cells against the same oxidative insult. This fact is not surprising, indeed in a previous study<sup>3</sup> we observed that the L-DOPA enhances the pro-oxidative effect of manganese and an antioxidant (N-acetyl-cysteine) is only able to partially revert its negative effects on PC12 cells. A similar enhancement of the pro-oxidative process has been also observed *in vivo*, in particular in the striatum of freely-moving rats treated with manganese and L-DOPA.<sup>29</sup> This observation has important implications about the role of nanoceria during L-DOPA treatment; in fact, the protective effect of nanoceria on MnCl<sub>2</sub> + L-DOPA-exposed cells confirms that the auto-oxidation of L-DOPA enhances the Mn-related oxidative stress.<sup>3</sup>

#### 4. Conclusions

The present work shows that ceria nanoparticles are effective for the treatment of neurodegenerative Parkinson like diseases induced by chronic manganese intoxication. For the first time the antioxidant capability of nanoceria has been tested in PC12 cells by using MnCl<sub>2</sub> instead of H<sub>2</sub>O<sub>2</sub>. The protective role of nanoceria depends on nanoparticles size and concentration and affects both the cells viability and metabolism; a nanoceria concentration of 20 µg/ml provides the highest antioxidant effect on cell cultures pre-treated with MnCl<sub>2</sub>, however to reach the maximum antioxidant effect in PC12 cells the nanoceria dimension and the concentration should be kept under 10 nm and 100 µg/ml, respectively. Nanoceria is also able to reduce the oxidative stress caused by auto-oxidation in a simultaneous treatment with L-DOPA, envisaging an innovative therapeutic application. Further studies are ongoing for a better understanding of the CeO<sub>2</sub> antioxidant biochemical mechanisms in the intracellular environment and a further *in-vivo* investigation is

necessary for exploring the potential role of these nanoparticles in the treatment of Parkinson like diseases.

### **Acknowledgements**

M.F. Casula, D. Loche are acknowledged for TEM characterization of the nanoparticles. A. Pinna acknowledges INSTM for financial support.

## References

- <sup>1</sup> P. M. A. Antony, N. J. Diederich, R. Kruger and R. Balling, *FEBS Journal*, 2013, **280**, 5981-5993.
- <sup>2</sup> A. W. Willis, B. A. Evanoff, M. Lian, A. Galarza, A. Wegrzyn, M. Schootman and B. A. Racette, *Am. J. Epidemiol.*, 2010, **172**, :1357-1363.
- <sup>3</sup> R. Migheli, C. Godani, L. Sciola, M. R. Delogu, P. A. Serra, D. Zangani, G. De Natale, E. Miele and M. S. Desole, *J. Neurochem.*, 1999, **73**, 1155-1163.
- <sup>4</sup> M. Aschner, K. M. Erikson, E. Herrero Hernández, and R. Tjalkens, *NeuroMol. Med.* 2009, **11**, 252-266.
- <sup>5</sup> J. J. Lee, Y. M. Kim, S. Y. Yin, H. D. Park, M. H. Kang, J. T. Hong and M. K. Lee, *Biochem. Pharmacol.* 2003, **66**, 1787-95.
- <sup>6</sup> A. N. Basma, E. J. Morris, W. J. Nicklas and H. M. Geller, *J. Neurochem.*, 1995, **64**, 825-32.
- <sup>7</sup> M. Y. Lee, E. J. Choi, M. K. Lee and J. J. Lee, *Nutrition Research and Practice*, 2013, **7**, 249-255.
- <sup>8</sup> B. M. Reddy and A. Khan, *Catal Surv Asia*, 2005, **9**, 155-171.
- <sup>9</sup> M. Dasa, S. Patilb, N. Bhargava, J. F. Kanga, L. M. Riedela, S. Sealb and J. J. Hickmana, *Biomaterials*, 2007, **28**, 1918-1925.
- <sup>\*0</sup> I. Celardo, J. Z. Pedersen, E. Traversa and L. Ghibelli, *Nanoscale*, 2011, **3**, 1-10.
- <sup>1\*</sup> F. Esch, S. Fabris, L. Zhou, T. Montini, C. Africh, P. Fornasiero, G. Comelli and R. Rosei, *Science*, 2005, **309**, 752-755.
- <sup>12</sup> A. Pinna, C. Figus, B. Lasio, M. Piccinini, L. Malfatti and P. Innocenzi, *ACS Appl. Mater. Interfaces*, 2012, **4**, 3916-3922.
- <sup>13</sup> A. Pinna, B. Lasio, M. Piccinini, B. Marmiroli, H. Amenitsch, P. Falcaro, Y. Tokudome, L. Malfatti and P. Innocenzi, *ACS Appl. Mater. Interfaces*, 2013, **5**, 3168-3175.
- <sup>14</sup> M. Stevanović, J. Savíc, Br. Jordović and D. Uskoković, *Colloids Surf. B Biointerfaces* 2007, **59**, 215-223.
- <sup>15</sup> L. Yang, G. Sundaresan, M. Sun, P. Jose, D. Hoffman, P. R. McDonagh, N. Lamichhane, C. S. Cutler, J. M. Perezc and J. Zweit, *J. Mater. Chem. B*, 2013, **1**, 1421-1431.
- <sup>16</sup> J. M. Dowding, T. Dosani, A. Kumar, S. Seal and W. T. Self, *Chem. Commun.* 2012, **48**, 4896-4898.
- <sup>17</sup> a) A. A. Athawale, M. S. Bapat and P. A. Desai, *J. Alloys Compd.* 2009, **484**, 211-217. b) S. Samiee and E. K. Goharshadi, *Mater. Res. Bull.*, 2012, **47**, 1089-1095.
- <sup>18</sup> G. Ciofani, G. Genchi, I. Liakos, V. Cappello, M. Gemmi, A. Athanassiou, B. Mazzolai and V. Mattoli, *Pharm Res.* 2013, **30**, 2133-45.
- <sup>19</sup> H. Suzuki, T. Toyooka, Y. Ibuki, *Environ. Sci. Technol.*, 2007, **41**, 3018-3024.

- <sup>20</sup> P. A. Serra, G. Rocchitta, G. Esposito, M. R. Delogu, R. Migheli, E. Miele, M. S. Desole and M. Miele, *Br. J. Pharmacol.*, 2001, **134**, 275-282.
- <sup>21</sup> S. Samiee and E. K. Goharshadi, *Mater. Res. Bull.*, 2012, **47**, 1089-1095.
- <sup>22</sup> M. S. Lord, M. S. Jung, W. Y. Teoh, C. Gunawan, J. A. Vassie, R. Amal and J. M. Whitelock, *Biomaterials*, 2012, **33**, 7915-7924.
- <sup>23</sup> M. I. Zaki, G. A. M. Hussein, S. A. A. Mansour and H. A. El-Ammawy, *J. Mol. Catal.*, 1989, **51**, 209-220.
- <sup>24</sup> Z. Zhang, L. Yu, W. Liu and Z. Song, *Appl. Surf. Sci.* 2010, **256**, 3856-3861.
- <sup>25</sup> S. Chen, Y. Hou, G. Cheng, C. Zhang, S. Wang and J. Zhang, *Biol. Trace Elem. Res.*, 2013, **154**, 156-166.
- <sup>26</sup> G. Wang, Q. Mu, T. Chen and Y. J. Wang, *J. Alloys Compd.*, 2010, **493**, 202-207.
- <sup>27</sup> S. Singh, T. Dosani, A. S. Karakoti, A. Kumar, S. Seal, W. T. Self *Biomaterials* 2011, **32**, 6745-6753.
- <sup>28</sup> N. Singh, C. A. Cohen and B. A. Rzigalinski, *Ann. N.Y. Acad. Sci.*, 2007, **1122**, 219-230.
- <sup>29</sup> P. A. Serra, G. Esposito, P. Enrico, M. A. Mura, R. Migheli, M. R. Delogu, M. Miele, M. S. Desole, G. Grella and E. Miele, *Br. J. Pharmacol.*, 2000, **130**, 937-45.

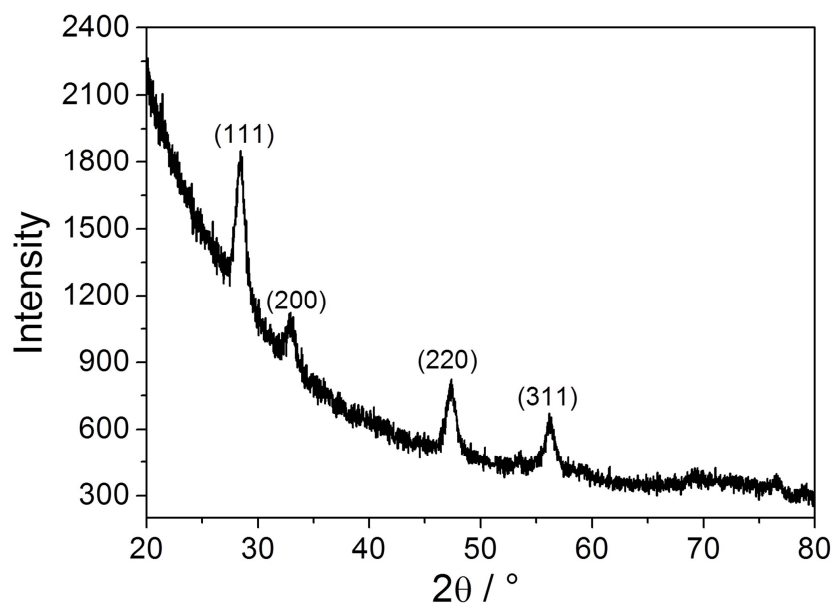


Figure 1

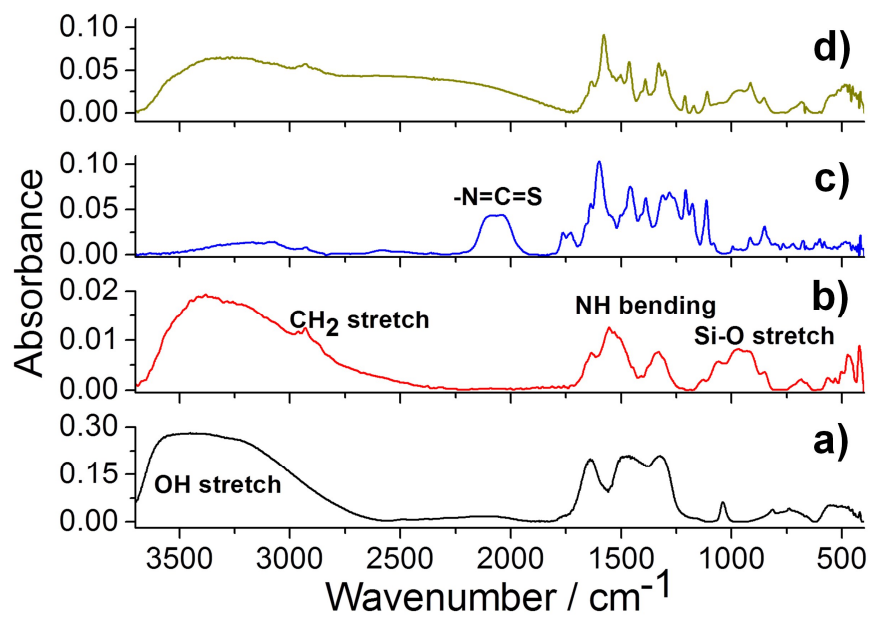


Figure 2

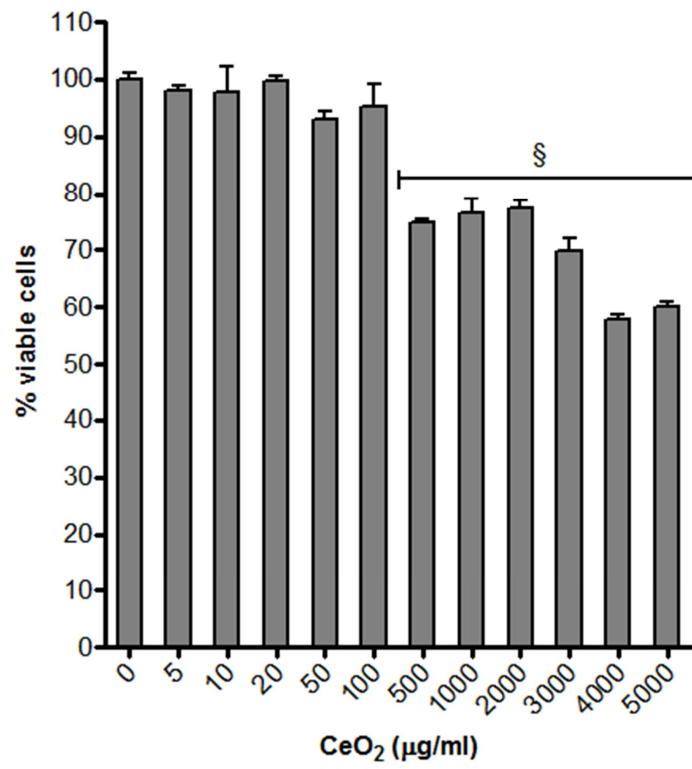


Figure 3

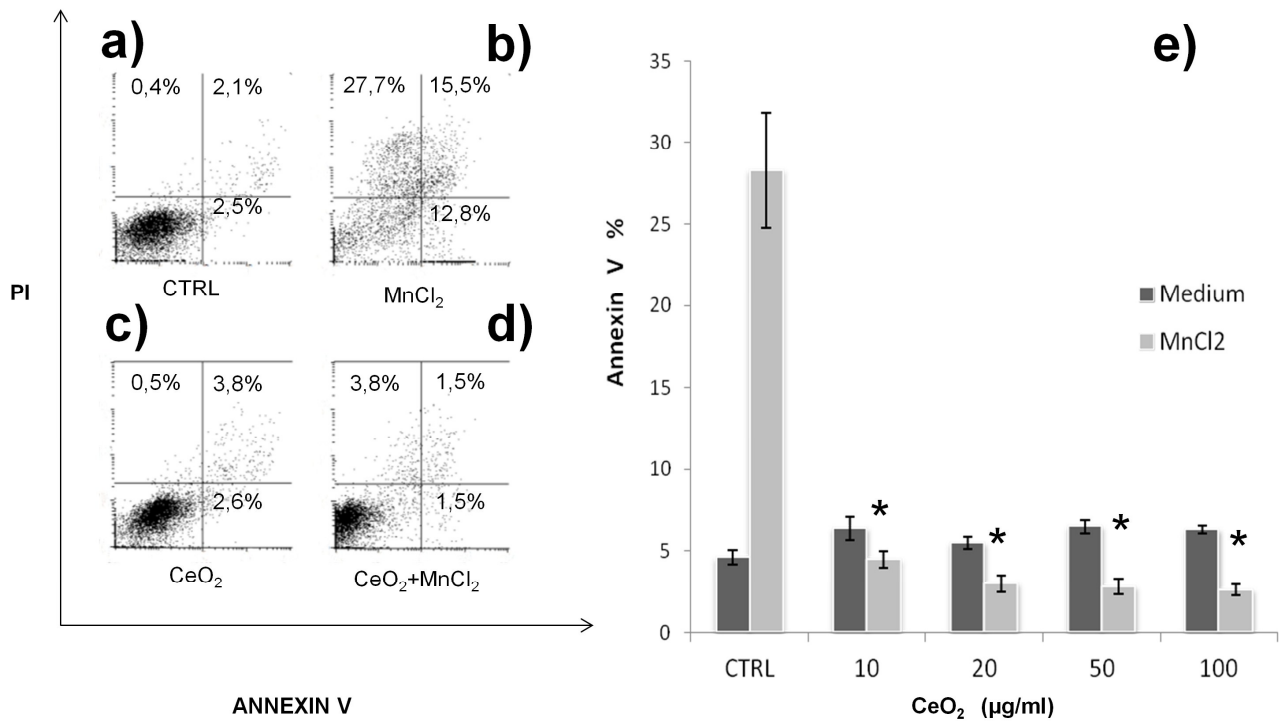
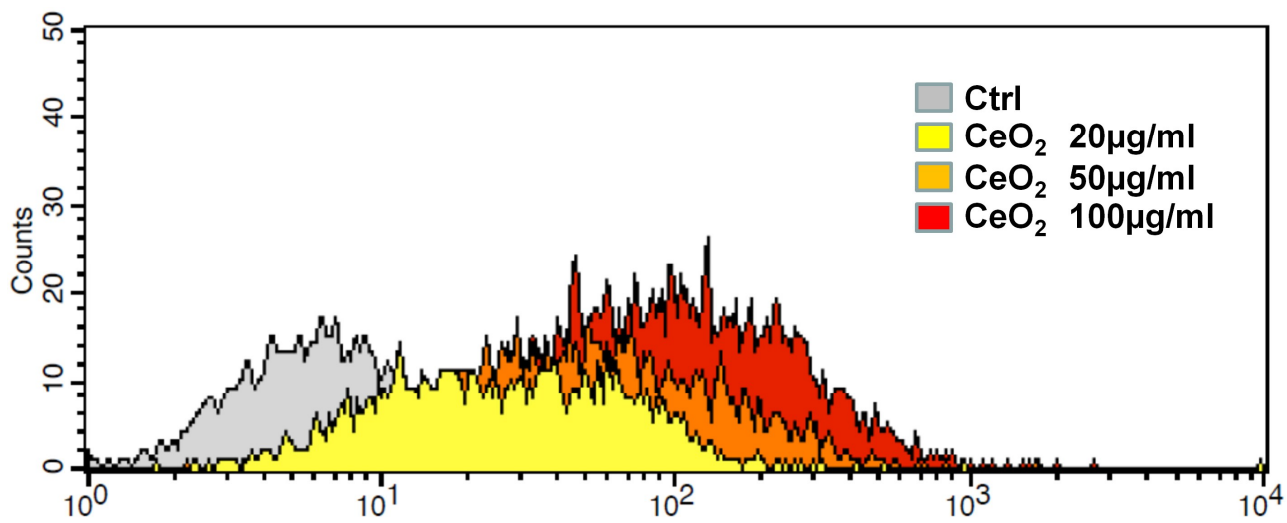


Figure 4

**Figure 5**

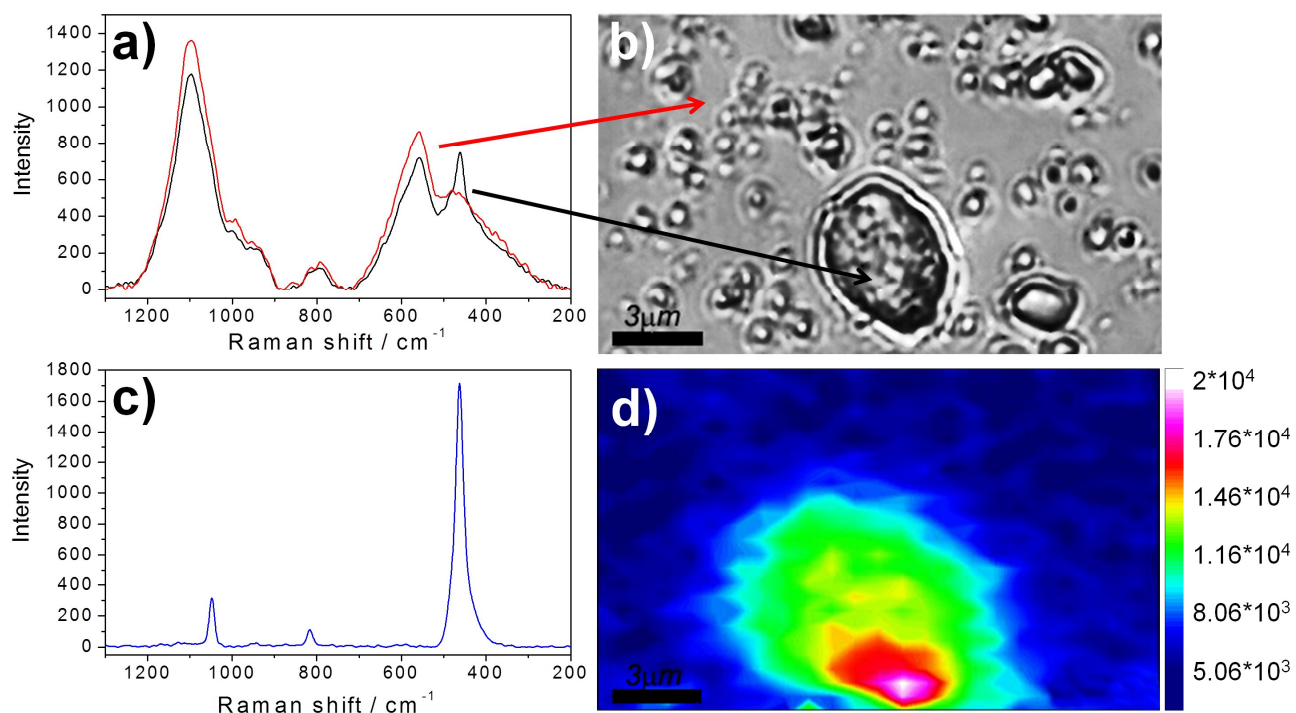


Figure 6

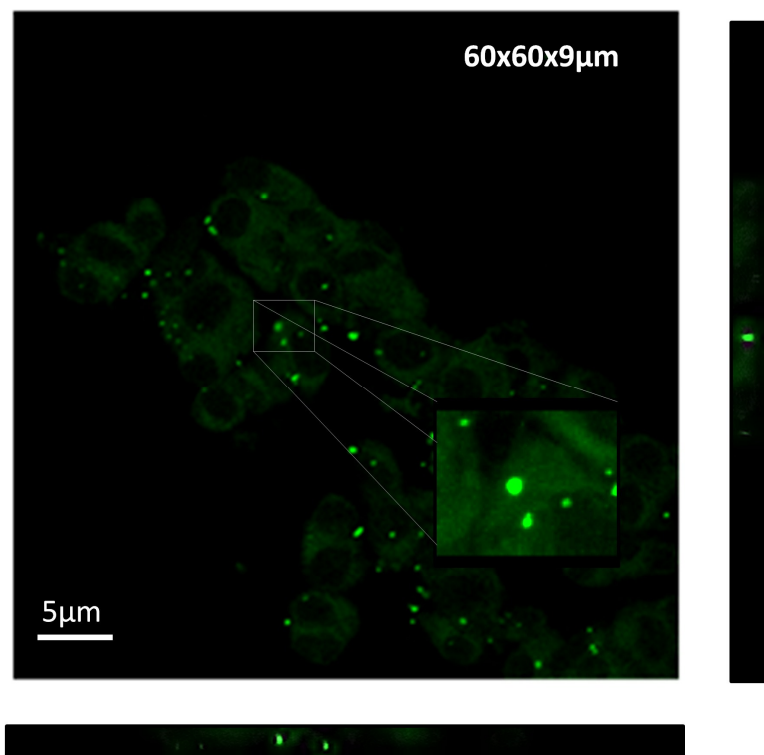


Figure 7

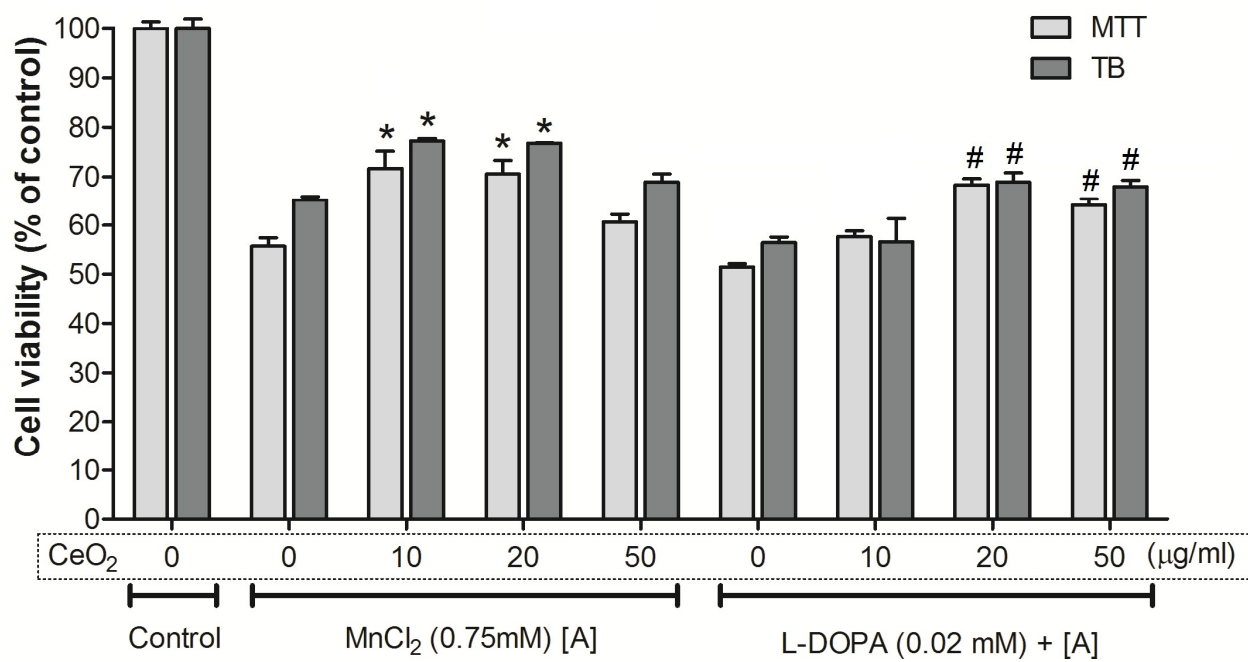


Figure 8

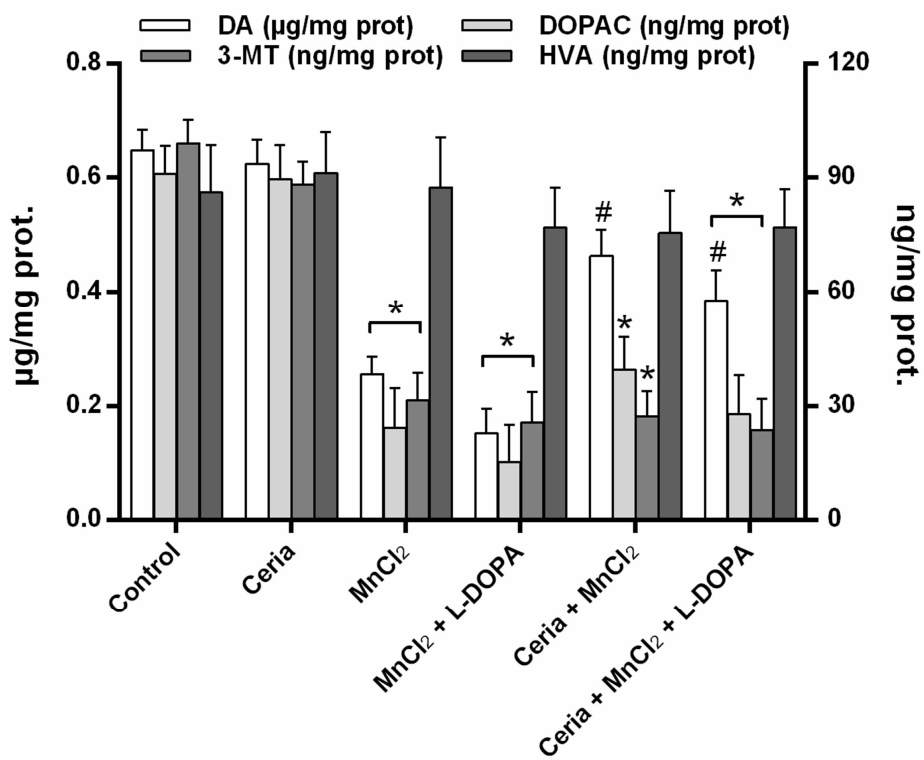


Figure 9

## Figure Captions

**Figure 1.** XRD pattern in the 20-80° 2 $\theta$  range of ceria nanoparticles synthesized by microwave treatment. The peaks have been indexed according to the cerianite structure.

**Figure 2.** FTIR absorption spectra in the 3700-400 cm<sup>-1</sup> range: a) ceria NPs (black line); b) nanoceria functionalized with APTES (red line); c) FITC (blue line) and d) nanoceria functionalized with APTES and FITC (green line).

**Figure 3.** The effect of nanoceria (5-5000  $\mu$ g/ml) on viability of PC12 for 48 h by MTT assay. § =  $p < 0.05$  versus control group.

**Figure 4.** Flow cytometry profile PI/annexinV performed on PC12 cell culture. a) PC12 control cells. b) PC12 cells treated with MnCl<sub>2</sub>. c) PC12 cells treated with nanoceria in a concentration of 20  $\mu$ g/ml and with MnCl<sub>2</sub> insult. d) PC12 cells treated with nanoceria. e) Average results of apoptotic PC12 cells treated with different concentration of nanoceria and exposed to MnCl<sub>2</sub> insult. Asterisks indicate statistically significant differences between CeO<sub>2</sub>-treated PC12 cells vs MnCl<sub>2</sub> CTRL ( $p < 0.01$ ).

**Figure 5.** Median fluorescence intensity (MFI) histogram of the cells as a function of the nanoceria concentration.

**Figure 6.** Raman imaging of PC12 cells incubated with nanoceria. a) Raman spectra in the 1300-200 cm<sup>-1</sup> range of extracellular environment (red line) and cellular environment (black line); b) optical image of single PC12 cell; c) Raman spectrum in the 1300-200 cm<sup>-1</sup> of ceria NPs in water

solution and d) Raman image obtained by integrating the active mode of cerium oxide at  $465\text{ cm}^{-1}$ . The integrated intensity is reported in false color scale.

**Figure 7.** 3D rendering through side projections of confocal Z-stack confirming ceria nanoparticles (green spots) internalization in PC12, as highlighted in the 4X zoom crop.

**Figure 8.** The effect of nanoceria on viability of cells treated with  $\text{MnCl}_2$  (0.75 mM) and  $\text{MnCl}_2$  + L-DOPA (0.75 mM + 0.02 mM) evaluated by MTT and trypan blue (TB) assays. Several concentrations of ceria nanoparticles have been used and the statistically significant relative protection has been calculated against  $\text{MnCl}_2$  alone ( $*=p<0.05$ ) and  $\text{MnCl}_2$  + L-DOPA ( $\#=p<0.05$ ).

**Figure 9.** Effects of nanoceria on manganese- and L-DOPA-induced changes in DA, 3MT, HVA and DOPAC concentrations in PC12 tissue after 48 h exposure. Results are the means  $\pm$  SEM of three experiments performed in triplicate.  $\# p<0.05$  versus  $\text{MnCl}_2$  group,  $* p<0.05$  versus control group.